

# Understanding pharmacokinetics using realistic computational models of fluid dynamics: biosimulation of drug distribution within the CSF space for intrathecal drugs

Andreas Kuttler · Thomas Dimke · Steven Kern ·  
Gabriel Helmlinger · Donald Stanski · Luca A. Finelli

Received: 5 November 2010 / Accepted: 11 November 2010 / Published online: 7 December 2010  
© The Author(s) 2010. This article is published with open access at Springerlink.com

**Abstract** We introduce how biophysical modeling in pharmaceutical research and development, combining physiological observations at the tissue, organ and system level with selected drug physiochemical properties, may contribute to a greater and non-intuitive understanding of drug pharmacokinetics and therapeutic design. Based on rich first-principle knowledge combined with experimental data at both conception and calibration stages, and leveraging our insights on disease processes and drug pharmacology, biophysical modeling may provide a novel and unique opportunity to interactively characterize detailed drug transport, distribution, and subsequent therapeutic effects. This innovative approach is exemplified through a three-dimensional (3D) computational fluid dynamics model of the spinal canal motivated by questions arising during pharmaceutical development of one molecular therapy for spinal cord injury. The model was based on actual geometry reconstructed from magnetic resonance imaging data subsequently transformed in a parametric 3D geometry and a corresponding finite-volume representation. With dynamics controlled by transient Navier–Stokes equations, the model was implemented in a commercial multi-physics software environment established in the automotive and aerospace industries. While predictions were performed *in silico*, the underlying biophysical models relied on multiple sources of experimental data and knowledge from scientific literature. The results have provided insights into the primary factors that can influence the intrathecal distribution of drug after lumbar administration. This example illustrates how the approach connects the causal chain underlying drug distribution, starting with the technical aspect of drug delivery

---

A. Kuttler · T. Dimke · S. Kern · D. Stanski · L. A. Finelli (✉)  
Modeling and Simulation, Novartis Pharma AG, Novartis Campus, 4056 Basel, Switzerland  
e-mail: luca.finelli@novartis.com

G. Helmlinger  
Modeling and Simulation, Novartis Institutes for Biomedical Research, Inc.,  
Cambridge, MA 02139, USA

systems, through physiology-driven drug transport, then eventually linking to tissue penetration, binding, residence, and ultimately clearance. Currently supporting our drug development projects with an improved understanding of systems physiology, biophysical models are being increasingly used to characterize drug transport and distribution in human tissues where pharmacokinetic measurements are difficult or impossible to perform. Importantly, biophysical models can describe emergent properties of a system, i.e. properties not identifiable through the study of the system's components taken in isolation.

**Keywords** Spinal cord injury · Intrathecal · Biophysics · Pharmacokinetics · Cerebrospinal fluid · Computational fluid dynamics · SCI · PK · CSF · CFD

## Introduction

With approximately 130,000 new cases per year globally, spinal cord injury is a global epidemic that typically involves males between the age of 16–30 in 82% of cases [1]. While there is no fully restorative cure for spinal cord injury yet, several new regenerative therapies targeting the spinal cord are being developed [1]. The development of one of these molecular therapies, namely anti-Nogo-A antibodies [2], has been the motivation for creating computational fluid dynamics (CFD) models to understand the pharmacokinetics (PK) of its delivery. The Nogo-A protein is an endogenous major neurite growth inhibitor leading to restricted axonal regeneration. Thus Nogo-A blockade with antibodies or peptides may enhance compensatory sprouting and neurite outgrowth. The primary site of action for the antibody is determined by Nogo-A expression on the cell surface of oligodendrocytes in the neighborhood of the injured section of the spinal cord which is typically located in the upper thoracic or cervical levels of the spine. Access to the spinal parenchymal tissue is challenged by the presence of inflammation due to the injury and the general protective nature of the tissues that surround the brain and spinal cord that keep foreign substances out. Thus delivery directly into the cerebrospinal fluid (CSF) in the spinal intrathecal space is likely necessary for these compounds.

A wealth of knowledge on delivery and PK of drugs targeting spinal cord function has been developed most notably with local anesthetics and opioids that are typically administered into the CSF in the spinal subarachnoid space by intrathecal injection or infusion at the lumbar site [3]. These agents are typically administered near the region where pharmacological effect in the spinal cord is needed, with the objective not to have the effect spread far from the administration site, particularly towards the upper regions of spinal cord and brain. Conversely, in cases like spinal cord injury where the relevant receptor target is located in the upper thoracic, the cervical, or even the brain region, a precise understanding of the influence of anatomy and physiology on pharmacokinetics is needed to optimize drug administration and provide drug distribution at this target site of pharmacologic action.

When modeling the pharmacokinetics of a drug administered intravenously in the systemic circulation, it is often assumed to be instantly well stirred within the central distribution volume, that it will reach its target site by rapid vascular

delivery and local diffusion, and that the processes of distribution and clearance will decrease drug concentration in a first order manner over time. These underlying assumptions enable description and understanding of systemically administered drugs with classical (compartmental) PK modeling approaches. In contrast, molecular transport and PK in non-well-stirred, oscillating fluid systems like the CSF following intrathecal drug administration may not be well described by classical PK modeling approaches due to poor validity of the assumptions above, which are normally reasonable for many drugs that show linear pharmacokinetics. A limitation to understanding human intrathecal PK of spinal cord injury therapies is imposed by intrinsic experimental difficulties and strong clinical restrictions to the number of and location where CSF samples can be taken, making direct and precise experimental observations possible only rarely at the lumbar site.

These differences motivate a series of questions for the pharmacometrician to address. *What is the drug concentration profile in the cervical spine region, following lumbar injection? Is there a distribution difference if the same dose is administered by slow infusion or instantaneous bolus injection? What are the most important factors affecting intrathecal distribution? Where does the rest of the drug go?* One alternative way to approach these questions is offered by the application of biophysical modeling of the spinal CSF system. Based on rich first-principle knowledge of fluid flow combined with experimental data at both conception and calibration stages, biophysical modeling may provide a novel and unique opportunity to interactively characterize detailed drug transport, distribution, and subsequent therapeutic effects in the CSF. Relying on the principles of momentum and mass conservation (Navier–Stokes equations) [4], a commercial multi-physics software environment established in the automotive and aerospace industries was used to understand the factors that contribute to drug distribution after injection into the intrathecal space.

After a brief introduction into the physiology of the cerebrospinal fluid system, we present the new methodology as well as the key mechanisms acting as driving forces on the fluid system that impact CSF pharmacokinetics. We conclude with an example of a detailed investigation of the intrathecal injection process, followed by a drug distribution simulation along the spinal CSF space over several hours, which at this stage might be considered as the two most immediate and useful model-based applications within the pharmaceutical drug development process.

## **Development of the CSF biophysical model**

### Theoretical and experimental constraints

Classical (compartmental) pharmacokinetic modeling of drug distribution in the cerebrospinal fluid is hampered by the assumptions underlying the method and is affected, particularly during the model-building phase, by the practical limitations in measuring drug concentration in the CSF along the spinal canal with sufficient frequency after injection. The general assumption of modeling compartments with spatially homogenous concentration of drug, while practically not accurate,

nonetheless allows the development of descriptive models after systemic drug administration that are representative of what one sees when measuring concentration levels in the blood. This is not necessarily the case for concentrations measured in the CSF, as noted by Kern et al. [5] in an analysis of the intrathecal pharmacokinetics of a peptide administered in a preclinical animal model. The temporal distribution pattern could be described by a series of exponential terms but equating the exponential terms to volumes and clearances did not result in values that had physiologic meaning.

Additionally, since access to the CSF is limited, the ability to sample the space to make measurements is a challenge. With the exception of specific experimental preclinical models where multiple catheters for drug delivery and concentration sampling can be made, the investigator is generally restricted to sample drug from the same catheter or needle that was used to deliver the drug. This can lead to sample contamination and relies on relatively fast drug dispersal after the injection. Otherwise, the sampling to measure the concentration could be the primary means by which drug leaves the CSF producing an artifact on the estimates of drug elimination from the space.

Because the CSF can be thought of as a closed space to some degree that is at positive pressure relative to other spaces in the body, fluid flow is impacted by punctures to the integrity of the dura, to positional changes of a patient, and a number of other physical factors which have been documented in clinical trials primarily with intrathecal anesthetic agents [6–8]. Despite these challenges, it is still important to understand what influences the duration and extent of drug exposure in the spinal subarachnoid space after intrathecal administration, which motivated our exploration using a computational fluid dynamics approach.

### From system anatomy to model geometry

Along the spinal column, the spinal cord and the CSF cavity are protected by the bones of the vertebral spine. The epidural space and the venous plexus are located in-between the vertebrae and the dura mater, which is the outermost resilient membrane covering the brain and the spinal cord. A middle layer (arachnoid mater) and the innermost membrane (pia mater) surround the brain, spinal cord and nerve roots. The CSF cavity in-between the arachnoid and dura mater is crossed by the outgoing nerve roots and various membranous elements in the posterior spinal subarachnoid space [9]. The shape of the spinal subarachnoid space is driven by the internal fluid pressure and its membrane structure, and by the surrounding bones and the epidural space [10]. This results in a non-homogenous annular volume with enhanced fluid space in the cervical and lumbar region, as well as a reduced cross-sectional diameter in the thoracic area [9].

The geometric model of the spinal subarachnoid space was based on data published in [11]. The region of interest in the current model was from cervical 1 (c1) to lumbar 2 (l2) (Fig. 1a, b). Cross-sections of the spinal subarachnoid space were approximated as elliptically-shaped areas that were connected via an axial spline. The area mesh was extruded along the dura and pia mater in the transverse direction, in order to get a hexahedral volume mesh. Additional local refinements

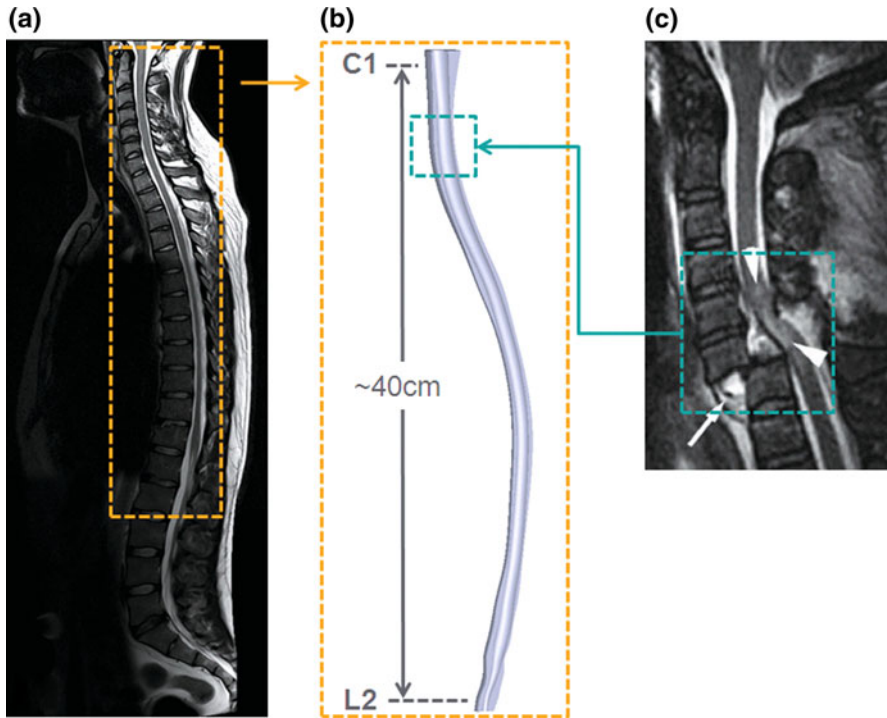


**Fig. 1** T2-weighted magnetic resonance images of the intact (a) and injured (c; C6/C7 dislocation) spinal cord; and (b) 3D reconstruction of the spinal CSF space used as model geometry

were introduced in areas with large diameters (e.g., upper cervical region) or with special physical conditions (e.g., lumbar injection region). Based on the results in [12], connective tissues, nerve roots and blood vessels (which form a meshwork within the spinal subarachnoid space) [9] were neglected in the current model.

#### From system physiology to model dynamics

The CSF, essentially an ultra-filtrate of the blood, surrounds the brain and spinal cord. CSF is produced mainly by the choroid plexus in the brain ventricles with a daily production rate of about 500 ml in humans [13]. The total volume of the CSF in humans is 170 ml on average, of which approximately 33% is found intracranially within the brain ventricles [14]. This volume shows large interindividual variability. From the ventricles, it flows through the foramina of Luschkae and the foramen of Magendie. A small percentage of CSF leaves the cranial space and enters the spinal subarachnoid space. Most of the CSF flows along the convexities of the surface of the brain toward the arachnoid granulations where it gets absorbed back into the venous circulation [13]. We approximated volume of the spinal canal to 50 ml.

The CSF motion in the spinal subarachnoid space may be described by a system of partial differential equations that conserve mass and momentum. The transient three-dimensional Navier–Stokes equations (Eqs. 1, 2) were solved with viscous

terms and molecular diffusion, using finite-volume (FV) computational fluid dynamics. Computations were performed using a commercial FV CFD solver, Starcd 3.26 (CD-Adapco).

$$\frac{\partial \rho}{\partial t} + \frac{\partial(\rho u)}{\partial x} + \frac{\partial(\rho v)}{\partial y} + \frac{\partial(\rho w)}{\partial z} = 0 \quad (1)$$

$$\frac{\partial \rho u}{\partial t} + \frac{\partial(\rho uu)}{\partial x} + \frac{\partial(\rho vu)}{\partial y} + \frac{\partial(\rho wu)}{\partial z} = -\frac{\partial p}{\partial x} + \left( \frac{\partial(\tau_{xx})}{\partial x} + \frac{\partial(\tau_{yx})}{\partial y} + \frac{\partial(\tau_{zx})}{\partial z} \right) + \rho \cdot f_x \quad (2a)$$

$$\frac{\partial \rho v}{\partial t} + \frac{\partial(\rho uv)}{\partial x} + \frac{\partial(\rho vv)}{\partial y} + \frac{\partial(\rho wv)}{\partial z} = -\frac{\partial p}{\partial y} + \left( \frac{\partial(\tau_{xy})}{\partial x} + \frac{\partial(\tau_{yy})}{\partial y} + \frac{\partial(\tau_{zy})}{\partial z} \right) + \rho \cdot f_y \quad (2b)$$

$$\frac{\partial \rho w}{\partial t} + \frac{\partial(\rho uw)}{\partial x} + \frac{\partial(\rho vw)}{\partial y} + \frac{\partial(\rho ww)}{\partial z} = -\frac{\partial p}{\partial z} + \left( \frac{\partial(\tau_{xz})}{\partial x} + \frac{\partial(\tau_{yz})}{\partial y} + \frac{\partial(\tau_{zz})}{\partial z} \right) + \rho \cdot f_z \quad (2c)$$

Under normal physiological conditions, the CSF behaves as an incompressible Newtonian fluid with the density and viscosity of water at 37°C. The diffusion constant of the drug compound investigated with this model (monoclonal antibody) was obtained from reference [15]. Biophysical parameters and dependent variables are listed in Table 1.

In the presented isotropic version of the Navier–Stokes equations, the density  $\rho$  and the cartesian velocity components  $u$ ,  $v$  and  $w$  determined the mass conservation Eq. 1. In addition the pressure  $p$  and the viscous shear stress tensor  $\tau_{ij}$  as well as the external acceleration forces  $f_i$  (e.g. gravity) were taken into account in the momentum conservation Eqs. 2a–2c.

### Driving forces

In addition to CSF circulation, production and absorption in the cranium, the spinal CSF dynamics are mainly driven by the pressure variation related to blood pulsation in the brain, as well as intrathoracic pressure variation generated by the diaphragm contraction in the abdominal space during breathing [16–18]. These two driving forces for fluid flow in the spinal canal were implemented in the model.

**Table 1** Model parameters and variables

Biophysical model parameters		
$\rho$ (kg/m <sup>3</sup> )	Density (37°C)	993.2
$D$ (m <sup>2</sup> /s)	Diffusion coefficient (from [15])	4.3e <sup>-11</sup>
$f_i$ (m/s <sup>2</sup> )	External acceleration vector (gravity)	[0, 0, -9.81]
Dependent variables		
$u, v, w$ (m/s)	Velocity components in $x, y, z$	
$p$ (Pa)	Pressure	
$\tau_{ij}$ (Pa)	Viscous shear stress tensor	

The brain is supplied by arterial inflow and venous outflow. Since the cranium is nearly rigid, the pulsation in blood flow must be accounted for. According to the Monro-Kellie hypothesis, this may be achieved via creating a compliant spinal canal [19]. As a result, an oscillating in- and outflow from/to the spinal canal is obtained. Alperin et al. [20] determined the transient mass flow profile in the cervical subarachnoid space of healthy volunteers and patients with Chiari malformation. The CSF velocities were obtained by velocity-encoded MRI. The cross-sectional averaged mass flow in the cervical region was applied as a periodic inlet condition representing the cranial blood volume changes.

The second driving force is a consequence of breathing [21]. With inhalation, the diaphragm increases the pressure in the abdomen; this also increases the venous pressure in the epidural space. The increased pressure leads to a compression of the spinal canal. In the current model, compression and expansion of the spinal subarachnoid space were implemented by moving the boundary of the space and by compressing the finite-volume mesh using a moving grid approach. The transient movement of the subarachnoid space acts like a second lower frequency pumping source for CSF transport.

The solution of the Navier–Stokes equations using the above-mentioned boundary conditions resulted in an oscillating fluid flow in the spinal canal. Peak fluid velocities on the order of 10 mm/s were obtained. Figure 2 shows velocities as vectors in a cross-section of the spinal canal (left: max amplitude caudal, right: max amplitude cranial).

Although the present calculations did not impose a net mass flow over the boundaries, a non-zero mean flow was obtained in the channel. Oscillatory flow inside complex geometries such as the annular volume of the spinal channel, with varying non-concentric cross-sections in the axial direction, may indeed generate secondary flow regions, a phenomenon known as steady streaming. Gaver and Grothberg described steady streaming in a tapered channel [22]. The effect of steady streaming resulting from an oscillating flow field on the given geometry is illustrated in Fig. 3.

### Simulating CSF motion

Transient simulations of oscillating fluids are computationally intensive. In the example described here, the computation of a single heart beat cycle would typically require over 12 h using a 2 Intel Xeon X5482 processor (12 MB cache, 3.2 GHz, 1600 MHz FSB). The reason for this is that impulse and mass conservation equations need to be solved for every oscillation cycle, which requires high resolution, both temporally and spatially. Hence, for the determination of concentration profiles several hours after an injection into the CSF, the method described above was not realistically applicable. Under the assumption that the pulsations are periodic, we determined the transport by steady streaming in one breathing cycle. With that we calculated the steady streaming velocity field, which was then kept constant (“frozen flow field”). Based on this frozen flow field, the molecular diffusion equation was solved, to determine molecular drug transport along the spinal space. The magnitude of steady streaming and the resulting drug

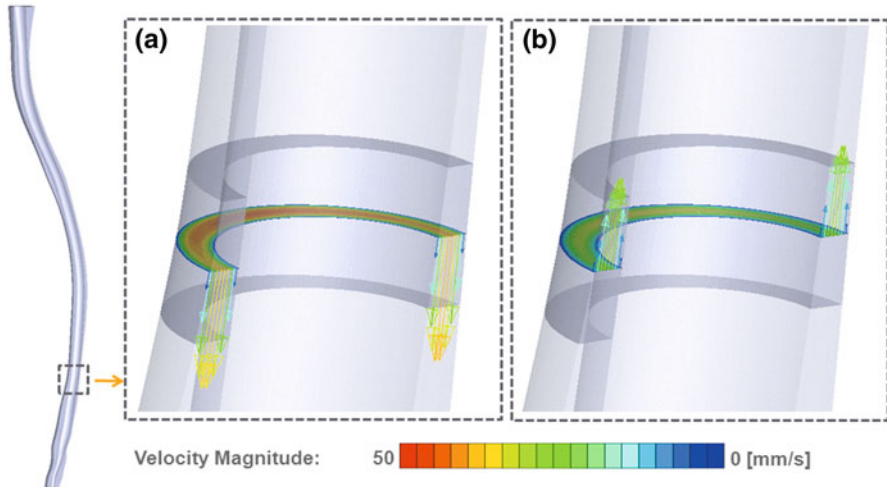


**Fig. 2** Maximum velocity flow profile in (a) caudal and (b) cranial direction at T10 during an oscillating flow simulation driven by pulsating pressure changes in the cranium and the abdominal space (contour plot of velocity magnitude shown on the complete cross-section, vector plot represented on a reduced subset of elements in the symmetry plane)

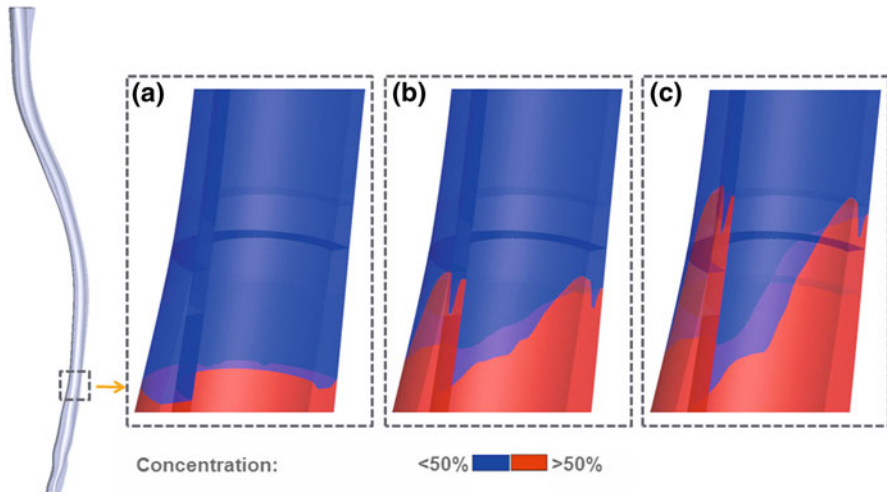


**Fig. 3** Simulation of drug transport starting at T11 (a) and propagating caudal in the lateral and cranial in the posterior and anterior region for five (b) and 10 s (c) using a steady streaming vector field previously determined by an oscillating fluid flow simulation (scaled to 50% of the initial concentration)

transport velocity was much lower than the oscillatory flow velocities. It was in the order of 0.1 mm/s, yet faster than molecular diffusion of large molecules such as monoclonal antibodies (MW ~ 150 kDa). This value was in general agreement with results from Di Chiro et al. [23] who showed that radiolabeled albumin injected into the lumbar CSF ascends the length of the spine to the base of the brain within 1 h. In



order to match this transport velocity, the wall motion amplitude, which generates the breathing oscillation, was adjusted accordingly.

### Applications of the biophysical model to better understand intrathecal pharmacokinetics

The biophysical model of the spinal CSF space described above allowed for the investigation of the principal transport mechanisms, a detailed analysis of injection and infusion processes, as well as the approximation of molecular drug concentration levels at certain time points post-injection. Two processes which are particularly relevant from a pharmacokinetic point of view: (i) an injection analysis, and (ii) a drug distribution simulation following a bolus injection are useful for illustrating insight from this modeling approach.

#### Intrathecal drug injection

In the context of a drug development project involving intrathecal administration of an anti-Nogo-A antibody at the lumbar level, we investigated the influence of both the needle injection angle and the administration rate on the concentration distribution and flow dynamics, during bolus injection. To this end, a submodel was created, focusing on the lumbar and lower thoracic regions with an additional inlet located at the level of L1-2 on the dura mater wall. To cope with the fluid dynamics generated by the injection jet, the computational grid within the injection region was refined, and a turbulence model (standard  $k-\epsilon$ -model) was introduced in this area [24]. Figure 4 visualizes the simulation results following an injection rate of

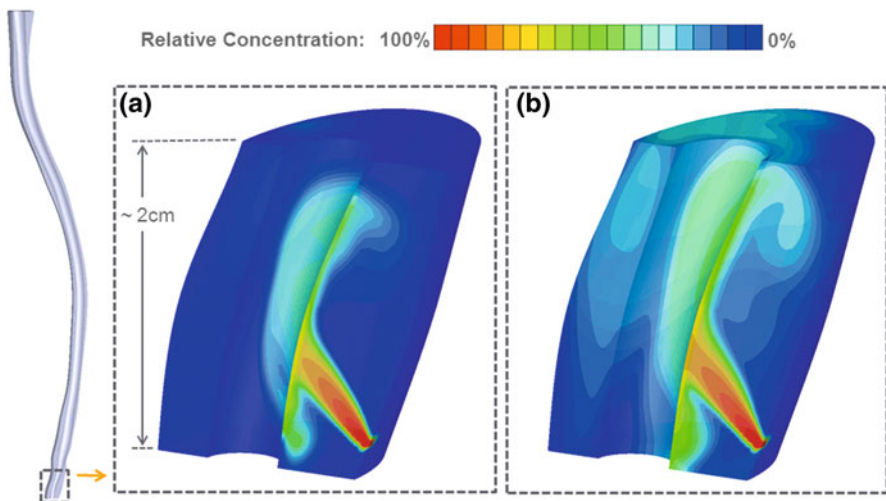


**Fig. 4** Simulation of an intrathecal injection (flow rate: 0.3 ml/s) at lumbar site L2 based on an oscillating CSF flow (a) 1 s and (b) 3 s after the start of the injection

0.3 ml/s and an injection angle of  $45^\circ$ . Local concentrations and the range of distribution in the oscillating CSF for different types of injection were characterized quantitatively in this manner.

In addition, the resulting drug distribution patterns could be used as a starting point for the determination of drug concentration levels at different positions along the spinal cord and over time.

#### Computing spinal drug distribution kinetics

The initial concentration distribution simulated above was now applied on the steady-transport field (steady-streaming). This is visualized for  $t = 0$  min,  $t = 10$  min and  $t = 20$  min, on an 11 cm segment of the lower thoracic lumbar region in Fig. 5.

The method described above was used to determine drug concentration levels within the complete canal over several hours. As an example, Fig. 6 shows the averaged concentration at different positions of the spinal subarachnoid space within the first hour after administration (right). In addition the contour plot (left side of the figure) illustrates the three-dimensional aspects of the distribution process 60 min after injection.

In the present simulations, neither drug binding to its receptor target nor drug metabolism was assumed. Both may nevertheless be considered as contributing to drug elimination in the CSF, via additional equations that can be integrated into the model. To address the final question regarding where the rest of the drug goes that enters the lower lumbar and sacral CSF space, an additional feature that estimated

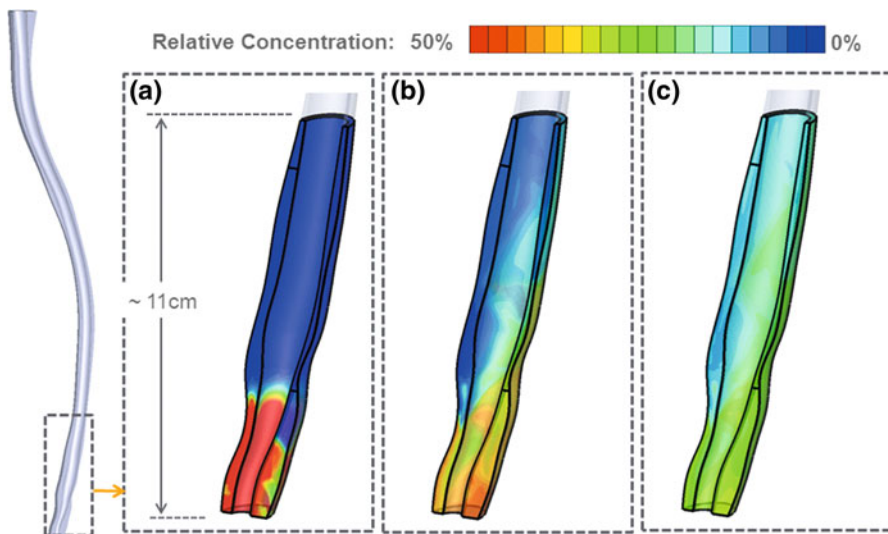


**Fig. 5** Three-dimensional drug propagation in the lower thoracic lumbar region starting from a concentration distribution simulated in a separate injection analysis (a). The contour plots (scaled to 50% of the initial concentration) after 10 min (b) and 20 min (c) show decreased and homogenized drug concentration levels

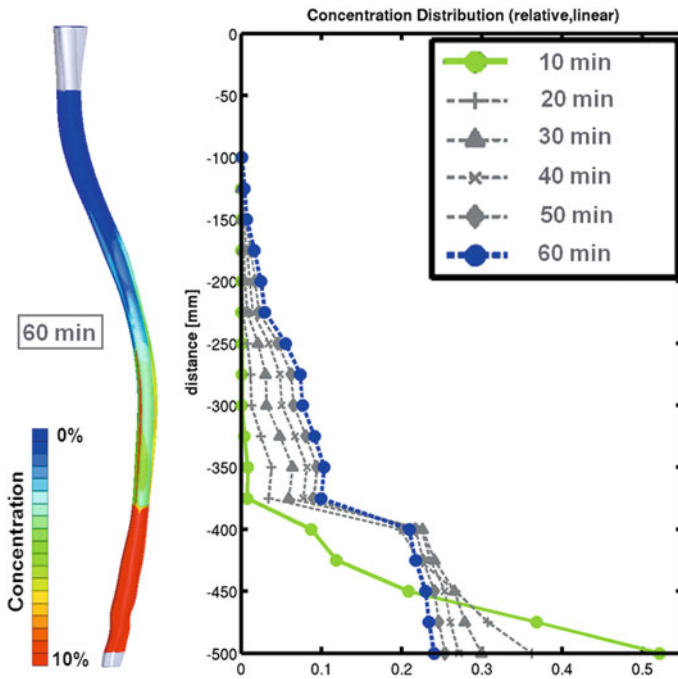


**Fig. 6** Steady streaming based transport simulation of an initial concentration distribution (determined in a separate injection analysis) in the spinal CSF (*left*: contour plot of the local concentration levels 60 min after the injection (scaled to 10% of the initial concentration); *right*: averaged drug concentration profiles from L2 to C4 within the first hour post-injection)

the remaining drug below the injection point was added to the model. The dynamics of fluid in this space was not explicitly included due to lack of literature data to inform the model. This missing information was determined during experimental validation to be applied in the future.

### Experimental validation

Since the computational model of CSF dynamics described here was developed from first principles based on the geometry of the spinal system and the physics of CSF flow, clinical literature was initially used for comparing the model predictions to measured fluid flow.

To gain direct physiological insight for the modeling of the spinal CSF space, a close collaboration with the MRI experts from the Division of Radiological Physics at the Institute of Radiology, University Hospital Basel was established. The group had previously developed a Breathing-ECG Synchronized System (BESSY) [25], which could be adapted to separately measure blood pulsation and respiratory influences on the CSF dynamics.

Results from initial cine MRI measurements for the oscillating CSF mass flow in the cervical region due to intracranial pressure changes were in the same order as what we determined in the cervical region using our model based on literature. As mentioned, those measurements were already performed by Alperin et al. [20] on large numbers of healthy volunteers and were published with high temporal resolution. In contrast, the amount of published data regarding the influence of breathing on the CSF dynamics was limited.

Our assumption on the dura mater motion for the presented model was originally based on information of CSF volume changes in the lumbosacral sac during increased abdominal pressure investigated by Martins et al. [17], as well as the transport measurements with radiolabeled albumin published by DiChiro et al. [23], which could not be explained without the additional effects of abdominal pressure changes due to breathing on the CSF dynamics. Using MRI image sequences of the CSF motion caused by breathing in a small study of healthy volunteers enabled us to refine those rough assumptions and provide another essential contribution in the understanding of the CSF dynamics.

For the planning of the experiments and the interpretation of the MRI sequences of the complex *in vivo* fluid oscillation, the biophysical model turned out to be a powerful tool to combine, compare and understand the imaging results in the environmental context. The 3D structure of the spinal CSF space in different positions could be generated semi-automatically from 240 high-resolution image slides. The resulting data from several velocity and tagging scans were applied and analyzed based on the predictions from the model. As a result, several discrepancies in the generated data could be identified and clarified even before the first fluid dynamic simulation of the complete system was started. This iterative investigation led to the synthesis of two final data sets of the spinal CSF space, based on two healthy volunteers, which included geometries from C1 to S5, transient flow patterns in cervical, thoracic and lumbar regions, as well as approximate values of the CSF dynamics generated during normal breathing. Velocity scans measured using cine MRI at several sections of the spine provided calibration for the simulated flow dynamics.

## Discussion and conclusions

We developed a 3D computational fluid dynamics model of the spinal canal, based on actual geometry reconstructed from MRI data and dynamics controlled by transient Navier–Stokes equations. The iterative model-building process allowed for a detailed investigation of the principal transport mechanisms observable in this system. The results from this approach of using realistic anatomical features coupled with biophysical principles of fluid flow dynamics and physiological characteristics of the cerebrospinal system have offered insights into the primary factors that can influence the intrathecal distribution of drug after lumbar administration. By providing an industry-unique framework for appropriate integration of biophysics first principles and clinical data into a dynamic system physiology platform, this technology allows for the simulation of different clinical

scenarios to support decision making, bringing model based-drug development to a next level.

Considering the limited number of CSF modeling examples in the literature and the stringent safety and ethical restrictions on experiments and clinical trials related to spinal cord injury, we were motivated to introduce a new quantitative assessment method of drug distribution in the CSF to help assess results from preclinical experiments and ongoing clinical trials, and combine them with physiological observations at the level of tissue-organ-system interactions and selected physiochemical properties. The goal was to understand factors that could affect the pharmacokinetics of a therapeutic antibody administered in the CSF, contributing to a greater understanding of therapeutic delivery for spinal cord injury.

One clinically relevant question that we could approach with the biophysical model described here was whether there is a practical distribution difference if the same dose and volume is administered by slow (more than 60 s administration time) or instantaneous (less than 60 s) bolus injection. Simulating these two administration scenarios revealed that initially the drug would move up the intrathecal space at different velocities, and that the orientation of the drug delivery needle relative to the CSF space would have an influence on axial dispersion of the drug, whereby maximally laminar flows would enhance axial dispersion of the injected drug and more turbulent flow would aid in circumferential dispersion [26]. However, when projected in the time scale of hours, those local differences would tend to dissipate, transport being dominated by the main driving forces of pulsation and breathing. These insights guided the clinical team when deciding on the clinical parameters of bolus administration to spinal cord injury patients enrolled in clinical trials, substituting to prior human dosing experimentation which would have been ethically difficult if not impossible to perform.

In a meta analysis by Fettes et al., [27] of factors that contribute to the success of spinal anesthesia, it was estimated that close attention to procedural detail by the anesthesiologist is likely the distinguishing factor between patients who received adequate spinal anesthesia and those who did not. Human clinical error can have a large impact on spinal anesthesia results within a population of clinicians who are commonly performing these types of treatments and assessments. Given that clinicians that have great experience in this procedure still produce variable results, there is need to better understand how drug is distributed throughout the CSF after intrathecal injection and what steps, if any, clinicians can take to use this effective drug delivery route more consistently.

The model of spinal CSF dynamics presented here allowed for the approximation of molecular drug concentration levels in the cervical spine following lumbar injection at certain time points post-injection as a function of biophysical, as well as injection parameters. Thus, differences in distribution over hours following either slow infusion or instantaneous bolus injection could be observed in the simulations [28]. These results suggested that bolus injection would not lead to an inferior distribution range compared to slow infusion. Because bolus injection delivers the total amount of drug to the lumbar injection site almost instantaneously, driving forces are likely to exert their effect on all drug molecules over a longer period of time, therefore increasing the chance for the drug to reach distant (cervical) targets

faster and with higher concentration. These results, although more qualitative in nature, provided the clinical team with useful confidence when deciding for bolus as the sole administration mode for later cohorts of ongoing clinical trials.

Predicting the amount of drug at a particular level of the spinal column after administration is difficult. Previous attempts to use classical pharmacokinetic approaches for modeling drug delivery in the cerebrospinal fluid have worked reasonably well for describing the dose–response relationship when the target site of drug effect is directly at the site of injection [29]. This has advanced the understanding and utility of spinal anesthesia for instance. However, when drug exposure after spinal administration occurs away from the site of injection, or the anticipated dose–concentration–effect relationship does not appear to hold, the limitations of the classical pharmacokinetic approach to spinal drug delivery become apparent. The further away the pharmacological target is from the site of administration, the more challenging it becomes to achieve a predictable concentration for attaining clinical effect. Reasons behind these difficulties were recently highlighted in an editorial by Drasner in the *British Journal of Anaesthesia* where he very colorfully recounts August Bier’s initial clinical report of spinal anesthesia with cocaine in 1899 [30]. Consistent in both Bier’s experiment and current clinical practice is the problem of variability in clinical response that limits our knowledge of cerebrospinal fluid drug delivery.

This editorial accompanied an article by Ruppen et al. [31, 32] who provide data from patients that received a spinal anesthetic that was either rated as successful (complete anesthesia) or not and then assessed the concentration of bupivacaine, the spinal anesthetic, to determine if a concentration—response relationship could be identified in the patients who did not produce complete spinal anesthesia. Their results show that the range of concentrations one can measure from CSF is very large (26–781 ng/ml in patients) and did not correlate with the success of the anesthetic state. This provides further confirmation that the intrathecal space does not behave as a well mixed volume and that measuring concentration in the CSF after injection to support a classical pharmacokinetic approach may not provide any meaningful data for analysis, or information for clinical decision making.

What are the most important factors affecting intrathecal distribution? With the challenges to interpreting the clinical data that exists for characterizing the dose–concentration–effect relationship in spinally administered agents, our approach for understanding the influence of biophysical forces on distribution appears to be well motivated. By approaching the problem from first principles, the contribution of physiologic forces due to breathing and cardiac cycles was predicted as a primary factor that allows a drug to distribute through the spinal canal. While this allows axial spread of the administered agent, our results show that subtle factors such as drug speed of injection, orientation of the injecting needle, and the amount of fluid administered will have a differentiating effect on the pattern of drug distribution in the CSF. Given the variability that can occur in the CSF distribution, it is not surprising that measured values within a population of patients may not have a strong correlation to either the amount of drug given, the patient’s response to the agent (if directly measurable like anesthesia) or to a number of other typical covariates that are commonly used to adjust patient dosage.

These results provided evidence that allow us to assess the factors, which contribute the most significantly to *variation* in the overall distribution. Using biophysics and properties of fluid motion based on Navier–Stokes equations, allows us to predict the general axial movement of drug within the CSF over time, however, the amount of drug present at any particular spinal cord level is difficult to determine and not likely to be uniformly distributed throughout the level. This provides considerable insight into the challenges of targeting drug delivery in the CSF to a distant site from the injection location and gives us a means for assessing ways to better reach our clinical target with therapeutic agents.

The refined model, updated using flow scans from MRI, allows us to address the motivating question of this project to understand the influence of CSF dynamics on the resulting drug concentration levels measured in sparse data from clinical trials. After first matching the model to the experimental transport results for big, non-binding and stable molecules like albumin published by DiChiro et al. [23], additional *in vivo* data of different-sized molecules with various target binding affinities will be fully integrated. Beyond the understanding of the principle mechanisms and sensitivities of drug transport in the spinal CSF cavity, prediction of individual dosing using imaging and computational methods could be feasible using this approach. The necessary experimental investigations (e.g., Positron Emission Tomography, MRI, etc.) as well as the extension of the model functionality (molecule binding, metabolism, etc.) are currently in progress.

**Acknowledgements** The authors would like to acknowledge the collaborative interaction with Klaus Kucher, M.D., PhD. and Donald Johns, M.D., Ph.D. of the Novartis Translational Medicine group and Professor Klaus Scheffler and Francesco Santini, Ph.D. of the Division of Radiological Physics at the Institute of Radiology, University Hospital Basel.

**Open Access** This article is distributed under the terms of the Creative Commons Attribution Noncommercial License which permits any noncommercial use, distribution, and reproduction in any medium, provided the original author(s) and source are credited.

## References

1. Thuret S, Moon LD, Gage FH (2006) Therapeutic interventions after spinal cord injury. *Nat Rev Neurosci* 7:628–643
2. Buchli AD, Schwab ME (2005) Inhibition of Nogo: a key strategy to increase regeneration, plasticity, and functional recovery of the lesioned central nervous system. *Ann Med* 37:556–567
3. Cousins MJ, Bridenbaugh PO, Carr DB, Horlocker TT (eds) (2008) *Neural blockade in clinical anesthesia and pain medicine*, 4th edn. Lippincott Williams & Wilkins, Philadelphia, PA
4. Schlichting H, Gersten K (2000) *Boundary-layer theory*, 8th edn. Springer, Heidelberg, ISBN 3-540-66270-7
5. Kern SE, Allen J, Wagstaff J, Shafer SL, Yaksh T (2007) The pharmacokinetics of the conopeptide contulakin-G (CGX-1160) after intrathecal administration: an analysis of data from studies in beagles. *Anesth Analg* 104:1415–1420
6. Swenson JD, Lee TH, McJames S (1998) The effect of prior dural puncture on cerebrospinal fluid sufentanil concentrations in sheep after the administration of epidural sufentanil. *Anesth Analg* 86:794–796
7. Bailey PL, Lu JK, Pace NL, Orr JA, White JL, Hamber EA, Slawson MH, Crouch DJ, Rollins DE (2000) Effects of intrathecal morphine on the ventilatory response to hypoxia. *N Engl J Med* 343:1228–1234

8. Bernards CM (2006) Cerebrospinal fluid and spinal cord distribution of baclofen and bupivacaine during slow intrathecal infusion in pigs. *Anesthesiology* 105:169–178
9. Hogan Q (1999) Gross anatomy of the human vertebral column. In: Yaksh TL (ed) *Spinal drug delivery*. Elsevier Science B.V, Amsterdam
10. Parkin IG, Harrison GR (1985) The topographical anatomy of the lumbar epidural space. *J Anat* 141:211–217
11. Loth F, Yardimci MA, Alperin N (2001) Hydrodynamic modeling of cerebrospinal fluid motion within the spinal cavity. *J Biomech Eng* 123(1):71–79
12. Stockman HW (2006) Effect of anatomical fine structure on the flow of cerebrospinal fluid in the spinal subarachnoid space. *J Biomech Eng* 128(1):106–114
13. Wong CA (2007) *Spinal and epidural anesthesia*. McGraw-Hill, Australia. ISBN-13:978-0-07-143772-1
14. Gomes JA, Bhardwaj A (2009) Normal intracranial pressure physiology. In: Irani DN (ed) *Cerebrospinal fluid in clinical practice*, pp. 19–25
15. Jain RK (1987) Transport of molecules in the tumor interstitium: a review. *Cancer Res* 47:3039–3051
16. Alperin NJ, Lee SH, Loth F, Raksin PB, Lichtor T (2000) MR-intracranial pressure (ICP): a method to measure intracranial elastance and pressure noninvasively by means of MR imaging: baboon and human study. *Radiology* 217(3):877–885
17. Martins AN, Wiley JK, Myers PW (1972) Dynamics of the cerebrospinal fluid and the spinal dura mater. *J Neurol Neurosurg Psychiatry* 35(4):468–473
18. Lee RR, Abraham RA, Quinn CB (2001) Dynamic physiologic changes in lumbar CSF volume quantitatively measured by three-dimensional fast spin-echo MRI. *Spine* 26:1172–1178
19. Monkri B (2001) The Monro-Kellie hypothesis: applications in CSF volume depletion. *Neurology* 56(12):1746–1748
20. Alperin N, Sivaramakrishnan A, Lichtor T (2005) Magnetic resonance imaging-based measurements of cerebrospinal fluid and blood flow as indicators of intracranial compliance in patients with Chiari malformation. *Neurosurgery* 103:46–52
21. Friese S, Hamhaber U, Erb M, Kueker W, Klose U (2004) The influence of pulse and respiration on spinal cerebrospinal fluid pulsation. *Invest Radiol* 39:120
22. Gaver DP, Grothberg JB (1986) An experimental investigation of oscillating flow in a tapered channel. *J Fluid Mech* 172:47–61
23. Di Chiro G, Hammock MK, Bleyer WA (1976) Spinal descent of cerebrospinal fluid in man. *Neurology* 26:1–8
24. Launder BE, Spalding DB (1974) The numerical computation of turbulent flows. *Comput Methods Appl Mech Eng* 3(2):269–289
25. Santini F, Scheffler K (2007) Assessment of respiration- and cardiac-related flow patterns of cerebrospinal fluid using balanced steady-state free precession and breathing-ecg synchronization. In: *Proceedings of the joint annual meeting ISMRM-ESMRMB*, Berlin, Germany
26. Finelli LA, Kuttler A, Dimke T, Helmlinger G (2007) A computational model of cerebrospinal fluid dynamics for predictive biosimulation. In: *37th Annual Meeting of the Society for Neuroscience*, San Diego, USA, November 3–7
27. Fettes PD, Jansson JR, Wildsmith JA (2009) Failed spinal anesthesia: mechanism, management, and prevention. *Br J Anaesth* 102:739–748
28. Finelli LA, Dimke T, Kern S, Gerner HJ, Helmlinger G, Kuttler A (2009) Computational 3D modeling of cerebrospinal fluid dynamics for simulation of distribution of drug delivery and distribution. In: *48th Annual Scientific Meeting of the International Spinal Cord Society*, Firenze, Italy, October 21–24
29. Shafer SL, Shafer A (1999) Spinal pharmacokinetics. In: Yaksh TL (ed) *Spinal drug delivery*. Elsevier, Amsterdam
30. Drasner K (2009) Spinal anesthesia: a century of refinement and failure is still an option. *Br J Anaesth* 102:729–730
31. Ruppen W, Steiner LA, Drewe J, Hauenstein L, Brugger S, Seeberger MD (2009) Bupivacaine concentrations in the lumbar cerebrospinal fluid of patients during spinal anaesthesia. *Br J Anaesth* 102:832–838
32. Steiner LA, Hauenstein L, Ruppen W, Hampl KF, Seeberger MD (2009) Bupivacaine concentrations in lumbar cerebrospinal fluid in patients with failed spinal anaesthesia. *Br J Anaesth* 102:839–844